THERMAL ANALYSES OF LED LIGHT BARS AND BACKLIGHT MODULES

M.-Y. Tsai* **C.-Y. Tang** **C.-E. Zheng**

Department of Mechanical Engineering
Chang Gung University
Taoyuan, Taiwan

Y.-Y. Tsai **C.-H. Chen**

Unity Opto Tech. Co.
New Taipei, Taiwan

ABSTRACT

The effects of various parameters, such as thermal properties of substrates, thermal interface materials (TIMs) and heat sinks on the thermal performance of the light emitting diode (LED) light bars and backlight module are investigated experimentally and numerically in terms of junction temperature (T_j) and thermal resistances from junction to air ($R_{j\text{-}a}$). The results show that the measured $R_{j\text{-}a}$ of the light bars by powering-on five LEDs in the test is different from one by powering-on only one LED, resulting from the extra heat coming from the adjacent LED packages affecting the T_j for the case of powering-on five LEDs. For the modules, $R_{j\text{-}a}$ is significantly reduced by using the heat sinks for all backlight modules, and aluminum and iron heat sinks do not show any obvious difference in heat dissipation along with any substrates and TIMs. Furthermore, both experimental and simulation results show that the thermal conductivity of the substrates are more important and dominant than TIM and heat sink for the $R_{j\text{-}a}$ of the backlight modules concerned, and also demonstrate that the thermal field for the local model can represent the one in full-scale backlight module.

Keywords: Light emitting diode, Backlight module, Junction temperature, Thermal resistance.

1. INTRODUCTION

The light emitting diode (LED), which features high color rendering index, environmental friendliness, low-power consumption, long lifetime, small form factor, and short response time, has been gradually replacing the conventional cold cathode fluorescent lamp (CCFL) as a backlight source in TV and computer monitors industry. However, the issues of the LED backlight bars (or modules) with high cost, high junction temperature, and low reliability have to be resolved before gaining full market penetration [1-4]. It is well known that high junction temperature in the LEDs would lead to the reliability problems, such as low quantum efficiency, wavelength shifts, short lifetime, and even catastrophic failures [4-7]. As a result, the heat dissipation for such LEDs becomes an important issue. Many research efforts have been put to improve the heat dissipation of LED modules in the literature. The heat dissipation of LED array with and without fins and fan was analyzed using a finite element simulation [8]. Thick-film insulated aluminum substrates with optimum thermal via were proposed to outpace thermal performance of LED module with metal core printed circuit board (MCPCB) [9]. The copper-core MCPCB with thermal via design was adopted to lower the thermal resistance of chip-on-board LED module [10]. A thermal analysis of a high-brightness LED array package assembly by various placement algorithms associated with experimental validation has been studied [11]. An electrical-thermal-luminous-chromatic model was proposed to predict the color properties of a phosphor-converted white LED package under its working temperature [12]. The effects of chip distance, number of chips, and driving current on the thermal resistance of LED module have been investigated [13]. Aluminum nitride insulation plate structure, instead of MCPCB with the dielectric layer, was proposed for

* Corresponding author (mytsai@mail.cgu.edu.tw)

DOI : 10.1017/jmech.2016.80
Copyright © 2016 The Society of Theoretical and Applied Mechanics
https://doi.org/10.1017/jmech.2016.80 Published online by Cambridge University Press

improving heat dissipation of an LED module [14]. In this study, to tackle the heat dissipation problem with the LED backlight module, the thermal performances of the LED light bars and backlight module are investigated experimentally and numerically in terms of substrate thermal properties, thermal interface materials (TIMs) and heat sinks.

2. METHODOLOGIES

2.1 Test Specimens

The materials and configurations of light-bar specimens are shown in Fig. 1 including LED light bar and cross sections of various LED substrates. In the specimen fabrication, commercial LED packages with a size of 5.7 × 3 × 1 mm consisting of an LED die, a leadframe, PPA (Polyphthalamide) and an encapsulant were mounted with a pitch of 8.5 mm on various 8 mm-wide, 55 mm-long strip substrates, shown in Fig. 1(a). It is specially noted that for measurement purpose the measured LED package (at the center) has to be independently powered with electrical wires, while the other four are connected in series with a jump wire. Three types of substrates: aluminum, printed circuit board, and flexible substrate (denoting Al, PCB, and Flex, respectively) shown in Fig. 1(b) are evaluated. Note that the flexible substrate is similar to PCB, but

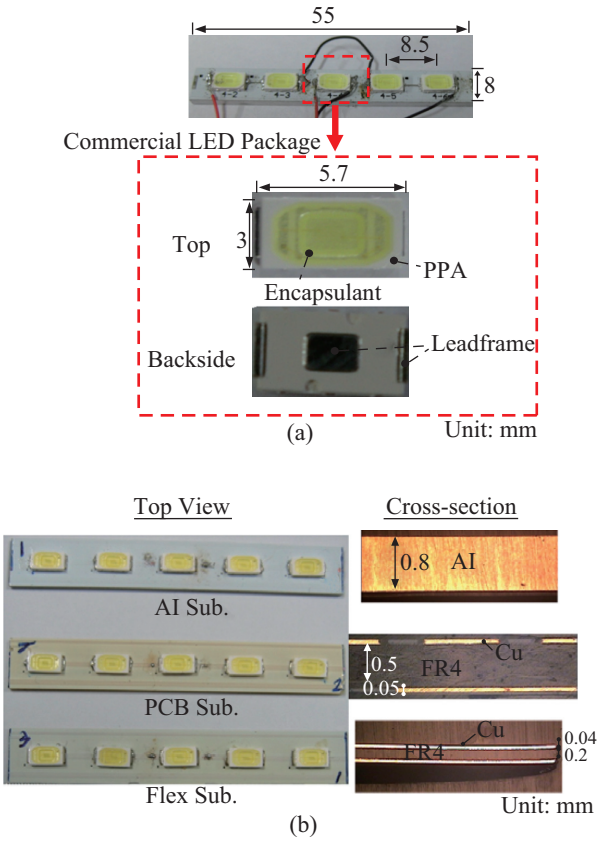


Fig. 1 Detailed materials and configurations of (a) LED packages on light bar and (b) with various substrates.

consists of two copper foils and one relatively thin FR4 layer. The configurations of LED backlight module are shown in Fig. 2(a) with various substrates, TIMs and heat sinks (including Al, aluminum, and Fe, iron), and Fig. 2(b) with a full model and a local model measuring 740 × 420 mm (with total 60 LED packages in two 330 mm-long light bars) and 60 × 55 mm (with 5 LED packages in one 55 mm-long light bar), respectively, for testing and analysis. The material thermal properties of the LED backlight modules are listed in Table 1.

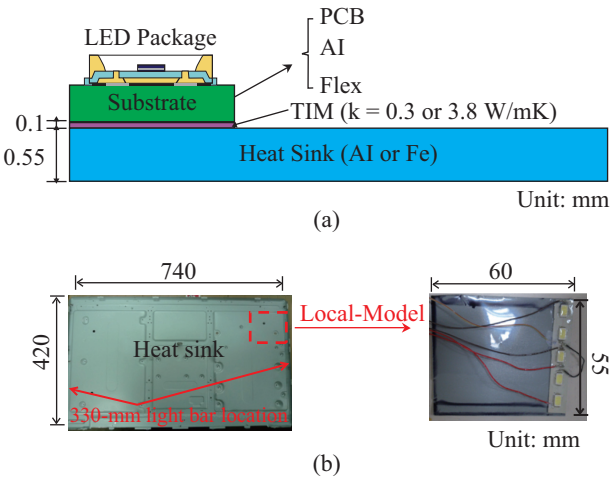


Fig. 2 (a) Schematic of LED backlight modules with various substrates, thermal interface materials (TIMs) and heat sinks, (b) a full model and a local model with the size of 740 × 420 mm (with total 60 LED packages along both sides) and 60 × 55 mm (with 5 LED packages), respectively.

Table 1 Thermal conductivities of materials used in the simulation.

Material Properties	Termal Conductivity k (W/mK)
LED Chip	42
Sapphire (Chip Sub.)	35
Silicone (Die Attach and Encapsulant)	0.3
PPA	0.3
Copper (Lead-Frame and Copper Foil)	380
Solder	49
Solder Mask (Substrate)	0.3
Aluminum (Substrate)	160
FR4	0.3
Iron	59

2.2 Junction Temperature Measurements

The chip junction temperature (T_j) was measured in this study by a junction temperature tester, which was developed on the basis of the principle of the electrical property of a diode with the linear relationship between

https://doi.org/10.1017/jmech.2016.80 Published online by Cambridge University Press

the electrical forward current and voltage [15]. The T_j measurement [16, 17] used here is in accordance with this principle by applying a small current (0.1 mA) to the LED. The calibration constant (β) in linear relationship in the LEDs can be determined in an oven calibration and then be used for correlating voltage change to temperature change. The pulse-current input is required for measuring the T_j. Before the T_j measurement, the driving current has to maintain the LED in power for about 30 minutes so as to ensure that the LED reaches a thermal steady state. The pulse current (0.1 mA) applied for temperature measurements is with only 1-msec duration for generating the LED voltage drop. This 0.1-mA current with 1-msec period of time is to avoid the current-induced thermal effect on the LED diode. During the measurement, the voltage drop between the initial-state voltage (V_{Mi}) and measurement-state voltage (V_M) is caused by the increase of T_j. Then the T_j can be described and determined by the following equations:

$$T_j = T_a + \Delta T_{j-a} \tag{1}$$

$$\Delta T_{j-a} = (V_{Mi} - V_M) \times \beta \tag{2}$$

where β is a calibration factor, T_a is air temperature, and $\Delta T_{j\text{-}a}$ is a temperature difference between the junction and air temperatures. The T_j tester was designed by the aforementioned principle. For easy interpretation of heat dissipation capability, the parameters of thermal resistances ($R_{j\text{-}a}$ and $R_{j\text{-}sub}$) are presented and defined as:

$$R_{j-a} = \frac{T_j - T_a}{P}; \quad R_{j-sub} = \frac{T_j - T_{sub}}{P} \tag{3.1; 3.2}$$

where P is an electrical input power.

The setup of the temperature measurement system is based on the JEDEC (the Joint Electron Device Engineering Council) specification [18] in which the transparent box is for avoiding excessive airflow that might cause measurement errors. As the LED light bar or backlight module reaches the thermal steady state, the surface temperatures are measured by the thermocouples attached on their substrate surfaces. There are three input powers (0.18 W, 0.26 W, and 0.4 W, corresponding to I = 60 mA, 80 mA, and 120 mA, respectively) used in the experimental measurements of both light bars and modules.

2.3 Thermal Simulations

The CFdesign, a commercial computational fluid dynamic code, was used for thermal simulation in this study. The three-dimensional computational fluid dynamic model shown in Fig. 3 was employed for eliminating the theoretical model limitations and iterative calculations of the convection coefficients due to the usage of the semi-empirical equations [19, 20]. The three equations of the fluid dynamics [21] from which the CFdesign code is derived, are applied to this numerical calculation by assuming the fluid is an incompressible flow, and expressed by:

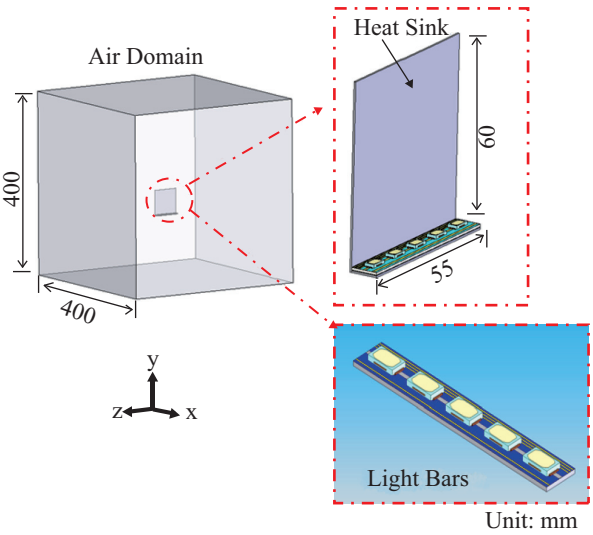


Fig. 3 Thermal modeling of the LED light bar and backlight module used in CFdesign analysis.

Continuity Equation:

$$\frac{\partial u}{\partial x} + \frac{\partial v}{\partial y} + \frac{\partial w}{\partial z} = 0 \tag{4}$$

Conservation of Momentum:
In the x-direction,

$$\frac{\partial u}{\partial t} + u\frac{\partial u}{\partial x} + v\frac{\partial u}{\partial y} + w\frac{\partial u}{\partial z} = -R\frac{\partial T}{\partial x} + \frac{\mu}{\rho}\left(\frac{\partial^2 u}{\partial x^2} + \frac{\partial^2 u}{\partial y^2} + \frac{\partial^2 u}{\partial z^2}\right) + f_u \tag{5.1}$$

In the y-direction,

$$\frac{\partial v}{\partial t} + u\frac{\partial v}{\partial x} + v\frac{\partial v}{\partial y} + w\frac{\partial v}{\partial z} = -R\frac{\partial T}{\partial y} + \frac{\mu}{\rho}\left(\frac{\partial^2 v}{\partial x^2} + \frac{\partial^2 v}{\partial y^2} + \frac{\partial^2 v}{\partial z^2}\right) + f_v \tag{5.2}$$

In the z-direction,

$$\frac{\partial w}{\partial t} + u\frac{\partial w}{\partial x} + v\frac{\partial w}{\partial y} + w\frac{\partial w}{\partial z} = -R\frac{\partial T}{\partial z} + \frac{\mu}{\rho}\left(\frac{\partial^2 w}{\partial x^2} + \frac{\partial^2 w}{\partial y^2} + \frac{\partial^2 w}{\partial z^2}\right) + f_w \tag{5.3}$$

Conservation of Energy:

$$\rho C_p\left(\frac{\partial T}{\partial t} + u\frac{\partial T}{\partial x} + v\frac{\partial T}{\partial y} + w\frac{\partial T}{\partial z}\right) = \frac{\partial}{\partial x}\left(k\frac{\partial T}{\partial x}\right) + \frac{\partial}{\partial y}\left(k\frac{\partial T}{\partial y}\right) + \frac{\partial}{\partial z}\left(k\frac{\partial T}{\partial z}\right) = S_T \tag{6}$$

where ρ is the density (kg/m^3), R is the specific gas constant, T is the temperature (°K), k is the thermal

https://doi.org/10.1017/jmech.2016.80 Published online by Cambridge University Press

conductivity (W/mK), u, v, w are components of the fluid velocity in the x-, y- and z-directions (m/s), f_u, f_v, *and* f_w are the velocity sources, C_p is the specific heat (J/kgK), S_T is the temperature source term and μ is the dynamic viscosity ($N\text{-}s/m^2$). Thermal properties of materials for the LED backlight modules are listed in Table 1, in which only the steady-state thermal analyses are all applied in this study. For avoiding the zero-fluid-velocity boundary effect, the size of constructed air domain is in general about 5 to 10 times larger than that of the test specimen. So the size of air domain used in this study is 400 × 400 mm (since the maximum length of the sample is about 55 mm). On nature-convention boundary conditions, the top surface of air domain is assigned with zero pressure difference in the flow outlet, while the other five surfaces of the domain are specified by assuming room temperature of 25°C and zero fluid velocity in the x-, y- and z-directions. The laminar flow within the domain is adopted in the steady-state analysis at initial temperature of 25°C. Three input powers (0.18 W, 0.26 W, and 0.4 W) with 75% conversion (which was determined with an integrating sphere optical system by separating optical and thermal powers from the electrical input power) into heat are applied in the CFdesign analysis.

The grid stability analysis of this thermal simulation was also performed and the convergence of data was evaluated. The results indicate that if the element number is less than 100k, then obtained temperature field is not stable and convergent, due to averaging out the thermal gradient over the large size of the element. On the other hand, if a large element number, such as 348k, is used, the calculation time increases significantly. Therefore, the optimally-adopted element number of this simulation in this study was a slightly larger than 100k for each backlight module. As a result, the obtained T_j result is within only 0.5% difference from that with 348k elements.

3. RESULTS AND DISCUSSION

3.1 Experiments

Thermal behaviors of the light bars and backlight module were measured and discussed in terms of the junction temperatures and thermal resistances as follows:

3.1.1 Thermal Behaviors of LED Light Bars

The junction temperatures (T_j) and substrate temperatures (T_{sub}) in various LED light bars with powering-on only one LED with different input currents are shown in Fig. 4(a) from the measurements. It is shown that both temperatures for those light bars increase linearly with the input currents (or powers). And T_j in the light bar with the PCB substrate are relatively higher than the ones with Al and Flex substrates, while T_{sub} shows no apparent difference with different substrates. By using thermal resistance definitions in the equations (3.1) and (3.2), the T_j and T_{sub} data can be converted into thermal resistances, $R_{j\text{-}a}$ and $R_{j\text{-}sub}$, as shown in Fig. 4(b). It is worth mentioning that $R_{j\text{-}a}$ includes heat conduction and convection, while $R_{j\text{-}sub}$ only is responsible for heat conduction. The results indicate that the light bars with Al and Flex substrates have the similar, lowest values of $R_{j\text{-}a}$ and $R_{j\text{-}sub}$, while the one with PCB substrate has the highest values. This implies that the use of Al substrate can lower $R_{j\text{-}a}$ by about 57%, compared with that using the PCB substrate.

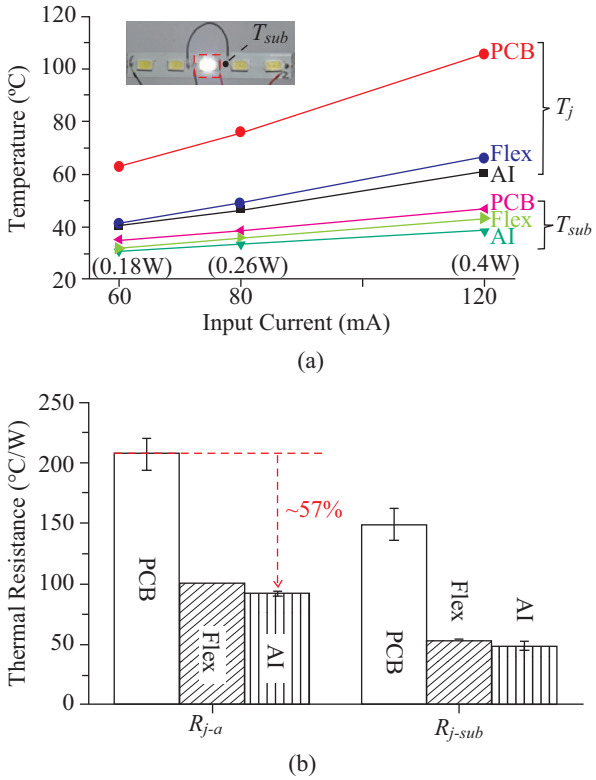


Fig. 4 (a)T_j and T_{sub} and (b)$R_{j\text{-}a}$ and $R_{j\text{-}sub}$ when powering-on one LED package on Al, PCB, and Flex light bars with various input powers, obtained from local-model experiments.

Furthermore, for the case of the light bars with powering-on five LEDs with different input currents, the T_j and T_{sub} are shown in Fig. 5(a) and the corresponding $R_{j\text{-}a}$ and $R_{j\text{-}sub}$ are presented in Fig. 5(b) from the measurements. These data of temperature and thermal resistance of the light bars for powering-on five LEDs share the similar trend with those from the case of powering-on one LED, except with an improvement of $R_{j\text{-}a}$ by only about 27%, rather than 57%, by using Al substrates instead of PCB substrate. The detailed comparison of $R_{j\text{-}a}$ for light bars with powering-on one and five LEDs is shown in Fig. 6 for closer examination. It indicates that for powering-on five LEDs (which would be more likely to be represented in a real application) the increase of $R_{j\text{-}a}$ for all light bars could result from the extra heat coming from the adjacent LED packages, which are neglected for the case of powering-on only one LED.

https://doi.org/10.1017/jmech.2016.80 Published online by Cambridge University Press

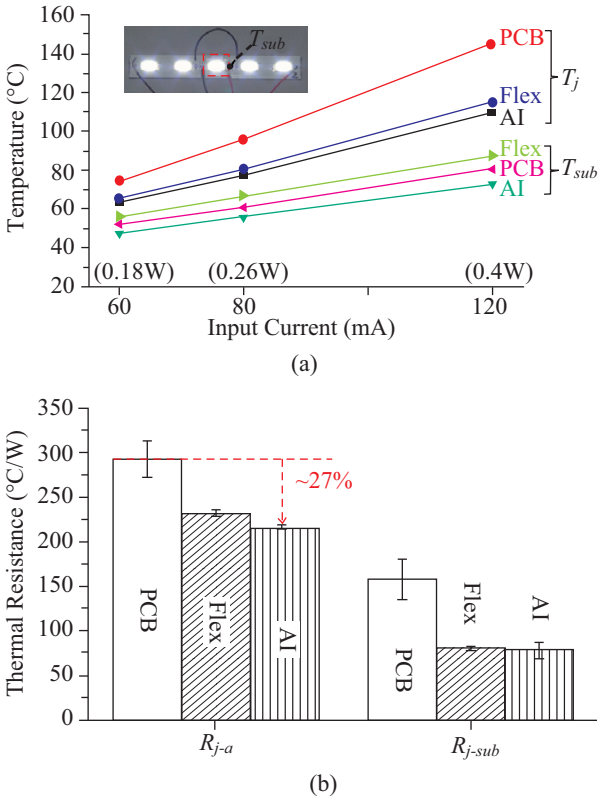


Fig. 5 (a)T_j and T_{sub} and (b)R_{j-a} and R_{j-sub} when powering-on five LED packages on PCB, Flex and Al light bars with various input powers, obtained from local-model experiments.

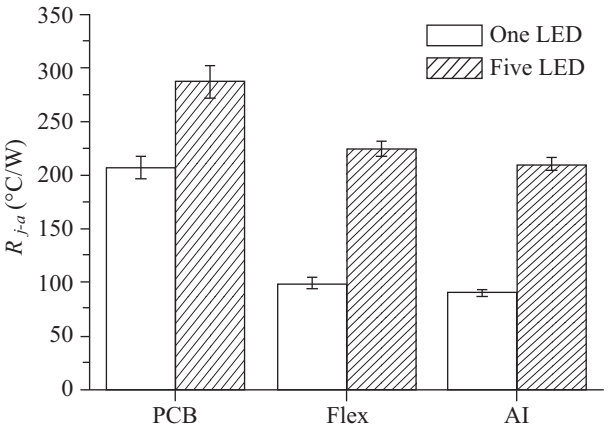


Fig. 6 Comparison of R_{j-a} with powering-on one and five LED packages on PCB, Flex and Al light bars, obtained from local-model experiments.

3.1.2 Thermal Behaviors of LED Backlight Modules

The T_j and T_{sub} in various LED modules with powering-on five LEDs with different input currents are shown in Fig. 7(a) from measurements in the local model with a TIM of k = 0.3 W/mK. It is shown that both temperatures for those modules increase linearly with the input currents (or powers). And T_j data in the module with the PCB substrate are relatively higher than the ones with Al and Flex substrates, while T_{sub} data show no apparent difference with different substrates. Besides, there is no obvious dissimilarity either for T_j or T_{sub} between the modules with the Al and Fe heat sinks. The T_j and T_{sub} data can be converted into thermal resistances, R_{j-a} and R_{j-sub}, as shown in Fig. 7(b). It is noted that R_{j-a} includes heat conduction and convection effects, while R_{j-sub} is only responsible for heat conduction. The results indicate that the backlight modules with Al and Flex substrates have the similar, lowest values of R_{j-a} and R_{j-sub} for both with Al and Fe heat sinks, whereas the one with PCB substrate has the highest values. This implies that, whether Al or Fe heat sink is applied, the use of Al or Flex substrate can lower the thermal resistance (R_{j-a}) by about 43%, compared with that using the PCB substrate.

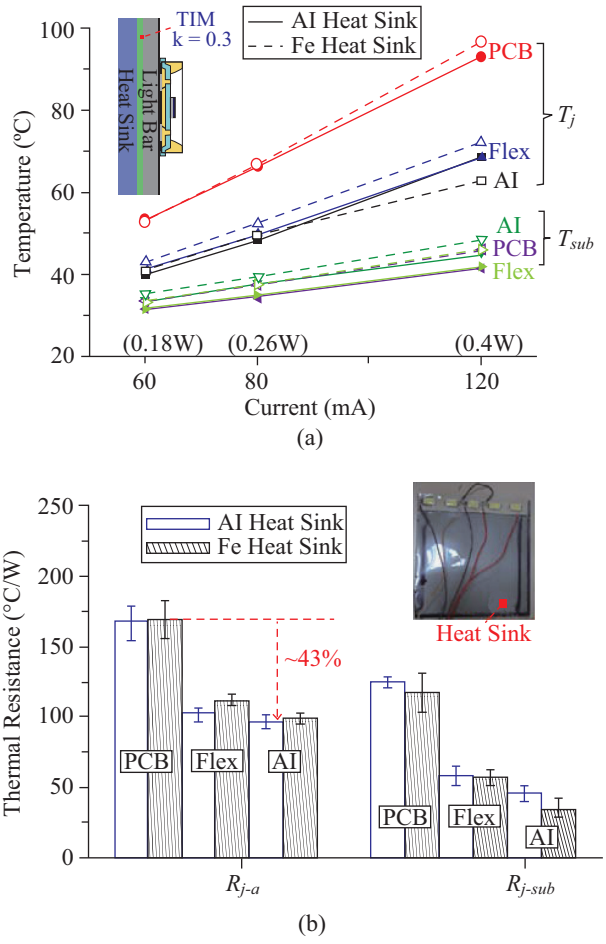


Fig. 7 (a)T_j and T_{sub} and (b)R_{j-a} and R_{j-sub} of LED backlight modules with powering-on five LEDs with different substrates and heat sink, obtained from local-model experiments.

Moreover, the R_{j-a} of backlight modules with different substrates, TIMs and heat sinks are shown in Fig. 8 in comparison with that without heat sink. The results indicate that R_{j-a} can be significantly reduced by using the heat sinks for all the cases; however, Al and Fe heat sinks do not provide any obvious difference in heat dissipation for any substrates and TIMs. Therefore, whether TIM is a good thermal conductor (with k = 3.8 W/mK) or bad one (with k = 0.3 W/mK) has no

https://doi.org/10.1017/jmech.2016.80 Published online by Cambridge University Press

apparent effect on the $R_{j\text{-}a}$ for the cases with PCB, Flex and Al substrates.

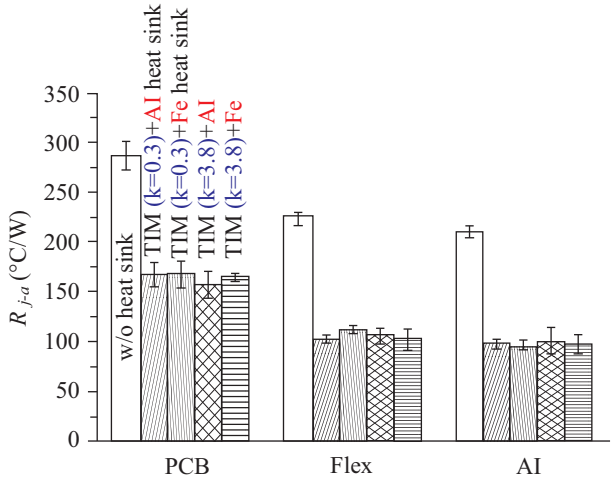


Fig. 8 $R_{j\text{-}a}$ of LED backlight modules with different substrates, TIMs and heat sinks, obtained from local-model experiments.

3.2 Simulations and Verification

To further gain more insights into thermal behavior of the light bars and backlight module, the thermal simulations by CFdesign have been carried out. The simulation results will be compared with those from experiments, and discussed in detail in terms of T_j and $R_{j\text{-}a}$.

3.2.1 Thermal Behaviors of LED Light Bars

The simulation results of T_j and $R_{j\text{-}a}$, as shown in Fig. 9(a) and (b) respectively, are compared with the experimental ones for the light bars. Note that error bars in the simulation results are for showing the deviation of the simulation results with three different input powers. It is found that both results are reasonably consistent in both quality and quantity, except with slightly higher values of $R_{j\text{-}a}$ predicted from the simulation, due to neglecting modeling the power wires (which provide additional heat-dissipation path) used for powering-on the LEDs during the T_j measurement. Despite the minor difference, the simulation model, as a result, has been proved to be feasible to predict the thermal behaviors of the light bars, even with slightly higher systematic value of $R_{j\text{-}a}$.

In order to improve the thermal behavior of the PCB light bar for cost reduction, the validated model associated with various thermal-via designs of PCB substrate shown in Fig. 10(a) was utilized and subject to the input power of 0.4 W per LED. The obtained results of T_j are compared with Al light bar. The results shown in Fig. 10(b) illustrate that the PCB substrate with thermal-via design can lower the T_j of the light bar, and the decrease of T_j become less apparent until 9 vias used. The T_j of this PCB light bar with 9 thermal vias can be lowered to 114°C by up to 31°C, close to the one with 108°C for the Al light bar. Furthermore, the detailed

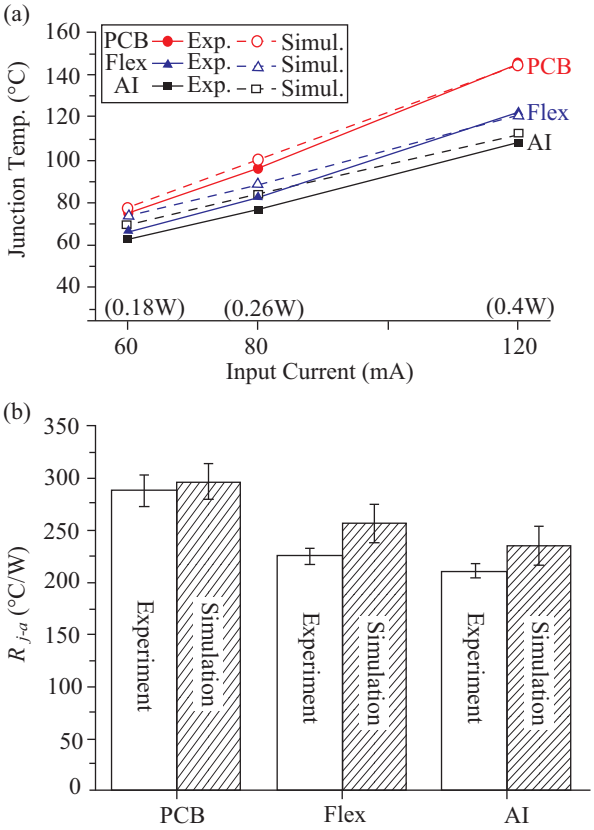


Fig. 9 Comparison of (a) T_j, and (b) $R_{j\text{-}a}$ of the light bars from simulation and experiments for powering-on five LED packages on PCB, Flex and Al substrates with various input powers.

thermal fields shown in Fig. 11 indicates that thermal gradient is noticeable from T_j to T_{bot} for the PCB light bar without via (with the temperature difference of about 55°C), but less obvious for one with 9 vias which has the temperature difference of only 12°C. It implies that the thermal-via design could provide the effective heat-dissipation path to enhance heat dissipation and thus to decrease the T_j, similar to the observation by [10]. Therefore, the PCB light bar with thermal-via design has the potential to be substituted for the Al light bar for cost-down purpose.

3.2.2 Thermal Behaviors of LED Backlight Modules

The $R_{j\text{-}a}$ of the modules with different substrates and heat sinks are shown in Fig. 12, obtained from experiments and simulation. Both consistent results imply the thermal conductivity of the substrates are more important and dominant than TIM and heat sink for the $R_{j\text{-}a}$ of the backlight modules. This mechanism can be further explained using Table 2, which shows thermal resistance for each layer, obtained from temperature gradient divided by a thermal power from the simulation. It is shown that, unlike from the substrate, thermal resistances either from TIMs or heat sinks contribute a negligible amount to the total resistance. The consistent results also indicate that the simulation model is good enough to be employed to predict the thermal behaviors of the LED backlight modules. Since the above-mentioned results are limited to the local model,

https://doi.org/10.1017/jmech.2016.80 Published online by Cambridge University Press

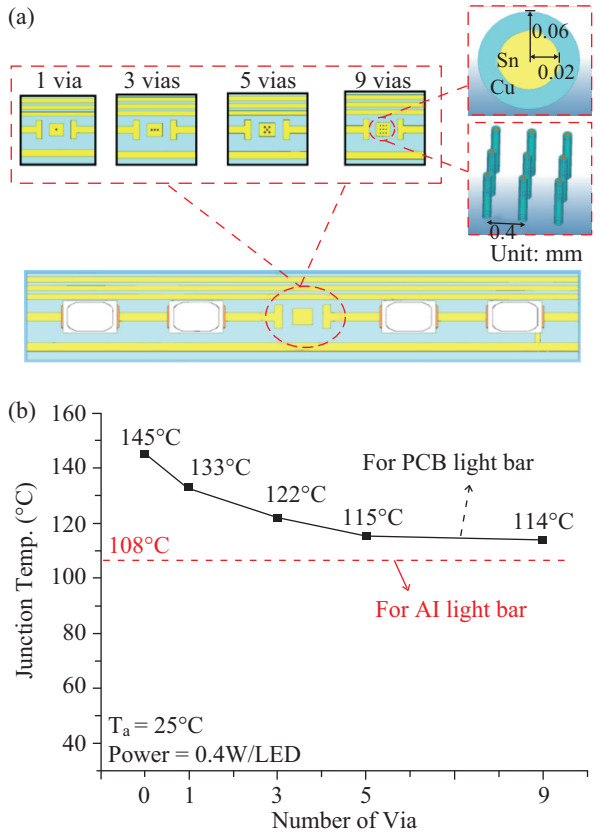


Fig. 10 (a) New design of PCB substrate with various numbers of thermal vias, and (b) the effect of via numbers in PCB substrate on T_j for the PCB light bar from simulation (with power = 0.4 W/LED), in comparison with Al light bar.

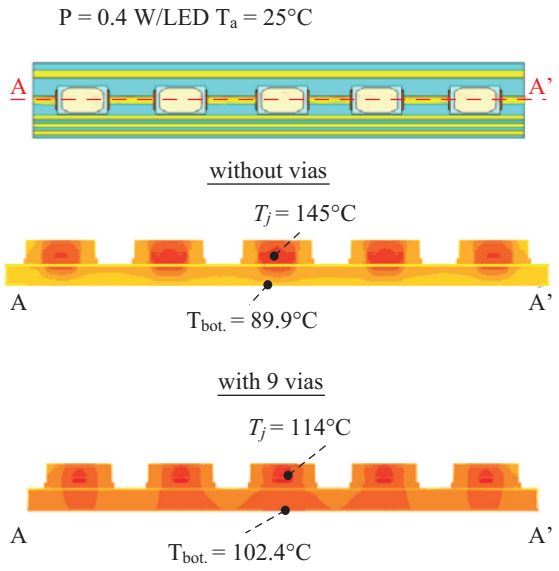


Fig. 11 Thermal fields for the PCB light bar without via and with 9 vias from simulation (with power = 0.4 W per LED).

it is interesting to understand the difference between local model and full model (which represents a real case). For checking whether the local model (with a

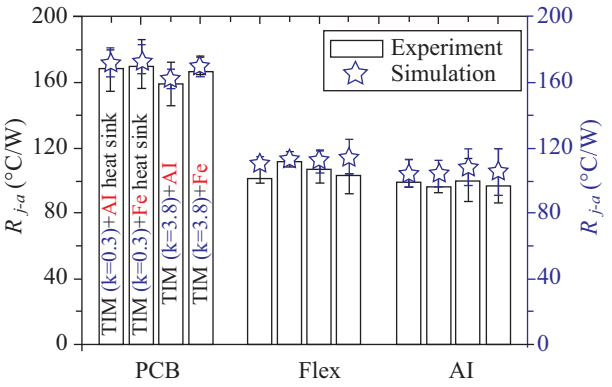


Fig. 12 Comparisons of $R_{j\text{-}a}$ of LED backlight modules with various substrates on Al and Fe heat sinks with TIMs (k = 0.3 and 3.8 W/mK), from experiment and simulation.

Table 2 Thermal resistance of each layer exacted from simulation.

Sub. \ R_{th}	$R_{pkg.}$	$R_{sub.}$	$R_{TIM(0.3)}$	$R_{TIM(3.8)}$	$R_{heat\ sink(Al)}$	$R_{heat\ sink(Fe)}$
Al Sub.	28.4	4.3	1.76	0.1	0.011	0.11
PCB Sub.	28.4	11.27	1.15	0.29	0.015	0.19
Flex Sub.	28.4	4.7	1.15	0.22	0.015	0.12

Unit: °C/W

5-LED light bar on a heat sink of 60 × 55 mm) could represent the full model (with a 30-LED light bar at each side on a heat sink of 740 × 420 mm), the temperature fields were analyzed by CFdesign for both cases under P = 0.4W per LED for a module with PCB substrate, TIM (k = 0.3 W/mK) and Al heat sink. The results shown in Fig. 13 indicate that temperature fields for both cases are consistent with each other either for T_j with less than 1% or surface temperatures with 2.5%. That implies the thermal field for the local model can successfully represent the one in a real case.

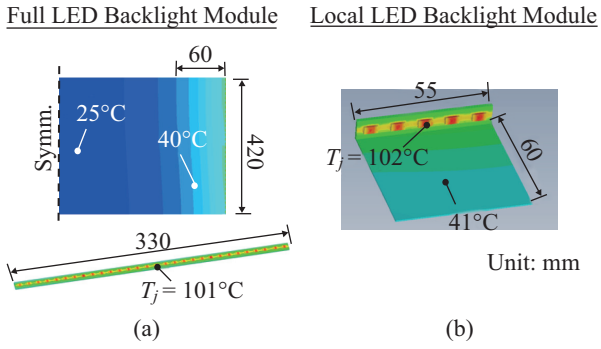


Fig. 13 Comparisons of simulation-obtained temperature fields of LED backlight modules between from (a) full and (b) local models under P = 0.4W per LED, with PCB substrate attached on Al heat sink with TIM (k = 0.3 W/mK).

https://doi.org/10.1017/jmech.2016.80 Published online by Cambridge University Press

4. CONCLUSIONS

The thermal performances of the light emitting diode (LED) light bars and backlight modules with various substrates, thermal interface materials (TIMs) and heat sinks, have been investigated experimentally and numerically in this study. The related junction temperature (T_j) and thermal resistances ($R_{j\text{-}a}$) for these LED light bars and modules have been obtained from experimental measurements and simulations. For the light bars, the increase of $R_{j\text{-}a}$ for all substrates and less improvement of $R_{j\text{-}a}$ using flexible or aluminum substrate instead of printed circuit board (PCB) substrate, were observed by powering-on five LEDs in the test, compared with those by powering-on only one LED. Those phenomena are attributed to the extra heat coming from the adjacent LED packages, which are ignored for the case of powering-on only one LED. It was experimentally found that $R_{j\text{-}a}$ can be significantly reduced by using the heat sinks for all backlight modules. And the use of aluminum or flexible substrate in backlight modules can lower the thermal resistance ($R_{j\text{-}a}$) by about 43%, compared with that using PCB substrate. It was also seen that aluminum and iron heat sinks do not provide any obvious difference in heat dissipation for any substrates and TIMs. Furthermore, the aforementioned experimental observations have been confirmed by the simulation, and both results show that the thermal conductivity of the substrates are more important and dominant than TIMs and heat sinks for affecting the $R_{j\text{-}a}$ of the backlight modules. The PCB substrate with thermal-via design, providing the effective heat-dissipation path to enhance heat dissipation, has proposed for replacing the aluminum substrate for cost-down purpose. It has also been successfully demonstrated that the thermal field for the local model can represent the one in full-scale LED backlight modules.

REFERENCES

1. Steranka, F. M. *et al*., "High Power LEDs Technology Status and Market Applications," *Physica Status Solidi (a),* **94**, pp. 380-388 (2002).
2. Arik, M., Petroski, J. and Weaver, S., "Thermal Challenges for the Future Generation Solid State Lighting Applications: Light Emitting Diode," *Proceedings of International Society Conference on Thermal Phenomena*, pp. 113-120 (2002).
3. Schubert, E. F. and Kim, J. K., "Solid-State Light Sources Getting Smart," *Science*, **308**, pp. 1274-1278 (2005).
4. Chang, M. H., Das, D., Varde, P.V. and Pecht, M., "Light Emitting Diodes Reliability Review," *Microelectronics Reliability*, **52**, pp. 762-782 (2012).
5. Narendran, N., Gu, Y., Freyssinier, J., Yu, P. H. and Deng, L., "Solid-state Lighting: Failure Analysis of White LEDs," *Journal of Crystal Growth*, pp. 449-456 (2004).
6. Narendran, N. and Gu, Y., "Life of LED-based White Light Sources," *IEEE/OSA Journal of Display Technology*, **1**, pp. 167-170 (2005).
7. Arik, M., Becker, C., Weaver, S. and Petroski, J., "Thermal Management of LEDs: Package to System," *Proceedings of SPIE*, **5187**, doi: 10.1117/12.512731 (2004).
8. Cheng, H. H., Huang, D. S. and Lin, M. T., "Heat Dissipation Design and Analysis of High Power LED Array Using the Finite Element Method," *Microelectronics Reliability*, **52**, pp. 905-911 (2012).
9. Juntunen, E., Sitomaniemi, A., Tapaninen, O., Persons, R., Challingsworth, M. and Heikkinen, V., "Thermal Performance Comparison of Thick-Film Insulated Aluminum Substrates With Metal Core PCBs for High-Power LED Modules," *IEEE Trans. on Components, Packaging and Manufacturing Technology*, **2**, pp. 1957-1964 (2012).
10. Juntunen, E., *et al.,* "Copper-Core MCPCB With Thermal Vias for High-Power COB LED Modules," *IEEE Transactions on Power Electronics*, **29**, pp. 1410-1417 (2014).
11. Yung, K. C., Liem, H., Choy, H.S. and Cai, Z.X., "Thermal Investigation of a High Brightness LED Array Package Assembly for Various Placement Algorithms," *Applied Thermal Engineering*, **63**, pp. 105-118 (2014).
12. Ye, H., *et al*., "Electrical-thermal-luminous-chromatic Model of Phos-phor-converted White Light-emitting Diodes," *Applied Thermal Engineering*, **63**, pp. 588-597 (2014).
13. Wang, C. P., *et al*., "Analysis of Thermal Resistance Characteristics of Power LED Module," *IEEE Transactions on Electron Devices*, **61**, pp. 105-109 (2014).
14. Jeong, M. W., Jeon, S. W., Lee, S. H. and Kim, Y., "Effective Heat Dissipation and Geometric Optimization in an LED Module with Aluminum Nitride (AlN) Insulation Plate," *Applied Thermal Engineering*, **76**, pp. 212-219 (2015).
15. Frank, R., "Semiconductor Junction Thermometers," *The Measurement Instrumentation and Sensor Handbook*, Webster, J. G. ed., CRC/IEEE Press, Boca Raton (1999).
16. Siegal, B., "Measurement of Junction Temperature Confirms Package Thermal Design," *LaserFocusWorld,* http://www.laserfocusworld.com (2003).
17. Tsai, M. Y., Chen, C. H. and Tsai, W. L., "Thermal Resistance and Reliability of High-Power LED Packages under WHTOL and Thermal Shock Tests," *IEEE Transactions on Components and Packaging Technologies*, **33**, pp. 738-746 (2010).
18. JEDEC Standard EIA/JESD51-2, "Integrated Circuits Thermal Test Method Environmental Conditions Natural Convection (Still Air)," (1995)
19. Tsai, M. Y., Chen, C. H. and Kang, C. S., "Thermal Measurements and Analyses of Low-Cost High-Power

https://doi.org/10.1017/jmech.2016.80 Published online by Cambridge University Press

LED Package," *Microelectronics Reliability*, **52**, p. 845-854 (2012).

20. Fu, Y. F., Yang, S. Y., Hung, T. Y., Lee, C. C. and Chiang, K. N., "Light Degradation Test and Design of Thermal Performance for High-power Light-emitting Diodes," *Microelectronics Reliability*, **52**, pp. 794-803 (2012).
21. Anderson, J. D., *Computational Fluid Dynamics*, McGraw-Hill International Editions, New York (1995).

(Manuscript received March 15, 2016,
accepted for publication May 11, 2016.)

https://doi.org/10.1017/jmech.2016.80 Published online by Cambridge University Press

https://doi.org/10.1017/jmech.2016.80 Published online by Cambridge University Press